

A pH Activated Configurational Rotary Switch: Controlling the *E/Z* Isomerization in Hydrazones

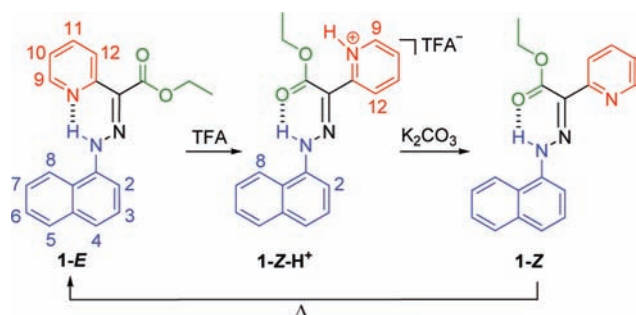
Shainaz M. Landge and Ivan Aprahamian*

Dartmouth College, Department of Chemistry, Hanover, New Hampshire 03755

Received November 2, 2009; E-mail: ivan.aprahamian@dartmouth.edu

Chemists, in the past two decades, have used creative and elegant design of molecules in their quest for discovering synthetic molecular machines¹ and switches² that can mimic macroscopic and biological analogues. Chemically activated³ rotary switches and motors have been actively pursued as they resemble rotary motors found in nature.⁴ One thing in common to all of these synthetic systems is that they rely on conformational changes in their function. Surprisingly, there seems to be a gap in the literature in the area of chemically controlled configurational⁵ rotary switches and/or motors. In contrast, photochemically driven configurational rotary switches have thrived, a process that led to the development of synthetic unidirectional rotary motors.⁶

Scheme 1. Acid/Base Controlled *E/Z* Isomerization of **1-E**



1,2,3-Tricarbonyl-2-arylhydrazones⁷ exist in solution as a pair of intramolecularly H-bonded hydrazone isomers^{8,9} that can equilibrate in the presence of catalytic amounts of acid or base.^{9c} This process results in the exchange of the relative positions of the substituents around the C=N bond, i.e., *E/Z* isomerization. However, these by no means entail full conversions from one isomer to another. Herein, we report the facile synthesis, characterization, and switching of the first (to the best of our knowledge) chemically activated configurational rotary switch. This original bistable system is based on a hydrazone building block, and pH¹⁰ is used to control the configuration around the C=N bond. We speculated that replacing one of the carbonyl groups in 1,2,3-tricarbonyl-2-arylhydrazones with a “proton acceptor” group such as pyridine will lead to a system that can be converted fully, effectively, and controllably from one isomer to the other by the consecutive addition of acid and base. In order to add another element of nonsymmetry into the system we decided to use a naphthylhydrazone derivative for the studies. This line of thought led to compound **1-E** (Scheme 1) that upon protonation affords **1-Z-H⁺**, which when treated with base yields the “metastable” **1-Z** configuration that thermally equilibrates back to **1-E**.¹¹

Hydrazone **1-E** was synthesized in a simple manner (see Scheme S1 in the Supporting Information): 1-Naphthylamine was treated with conc. HCl in H₂O and then with NaNO₂ at 0 °C to give 1-naphthalenediazonium chloride. In a separate flask ethyl-2-pyridylacetate was treated at 0 °C with sodium acetate in EtOH/

H₂O (5:1). These two solutions were combined and stirred at 0 °C for 1 h and then overnight at RT. After filtration, the crude product was subjected to column chromatography (SiO₂: CH₂Cl₂:Hexane, 1:1) to give **1-E** as a light-orange solid in 75% yield. ESI-MS revealed a peak at *m/z* 319.1 corresponding to the molecular ion.

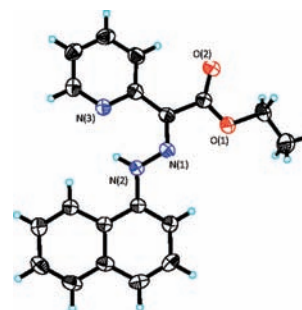


Figure 1. ORTEP drawing (50% probability ellipsoids) of **1-E**. The protons are placed in calculated positions.

The structure of **1-E** (Figure 1) has been unambiguously confirmed using X-ray crystal structure analysis. The structure is almost planar,¹² and the H-bonding between the N–H proton and the pyridine nitrogen subunit is apparent. The compound also adopts a conformation in which the naphthalene bay is oriented toward the N–H proton.

The ¹H NMR spectrum of **1-E** (Figure 2a) in CD₃CN shows a characteristic H-bonded N–H resonance at 15.8 ppm, in addition to the expected aromatic and aliphatic signals. The N–H chemical shift is in line with the pyridine nitrogen being H-bonded with the N–H proton. When the H-bonding is with an ester carbonyl, then the chemical shift is usually in the 12.5–14.5 ppm range.^{9d} A careful look at the ¹H NMR spectrum (see Figure S1 in the Supporting Information) shows a small signal at 12.8 ppm, stemming from the minor **1-Z** configuration. The integration of these two N–H resonances shows that the *E:Z* ratio in solution is 97:3.¹³ Calculated geometries¹⁴ (B3LYP/cc-pVDZ level of theory)^{15,16} of the two configurations in CD₃CN show that **1-E** is more stable by 2.7 kcal/mol than **1-Z**, which is in agreement with the isomer ratio observed in the ¹H NMR spectrum.

To gain further insight into the structure of **1-E**, we conducted 2D NMR spectroscopy studies and fully characterized the ¹H NMR spectrum. Interestingly the 2D NOESY experiment (see Figure S2 in the Supporting Information) shows a correlation between the N–H signal and the naphthalene H8 proton. This interaction indicates that the naphthalene subunit in **1-E** adopts the same conformation in solution as that observed in the solid state.¹⁷ 1D NOESY experiments (see Figures S3 and S4 in the Supporting Information) show correlations between the pyridine H9 proton and the N–H and naphthalene H8 protons. These NOE correlations conclusively show that **1-E** is the predominant configuration in solution.

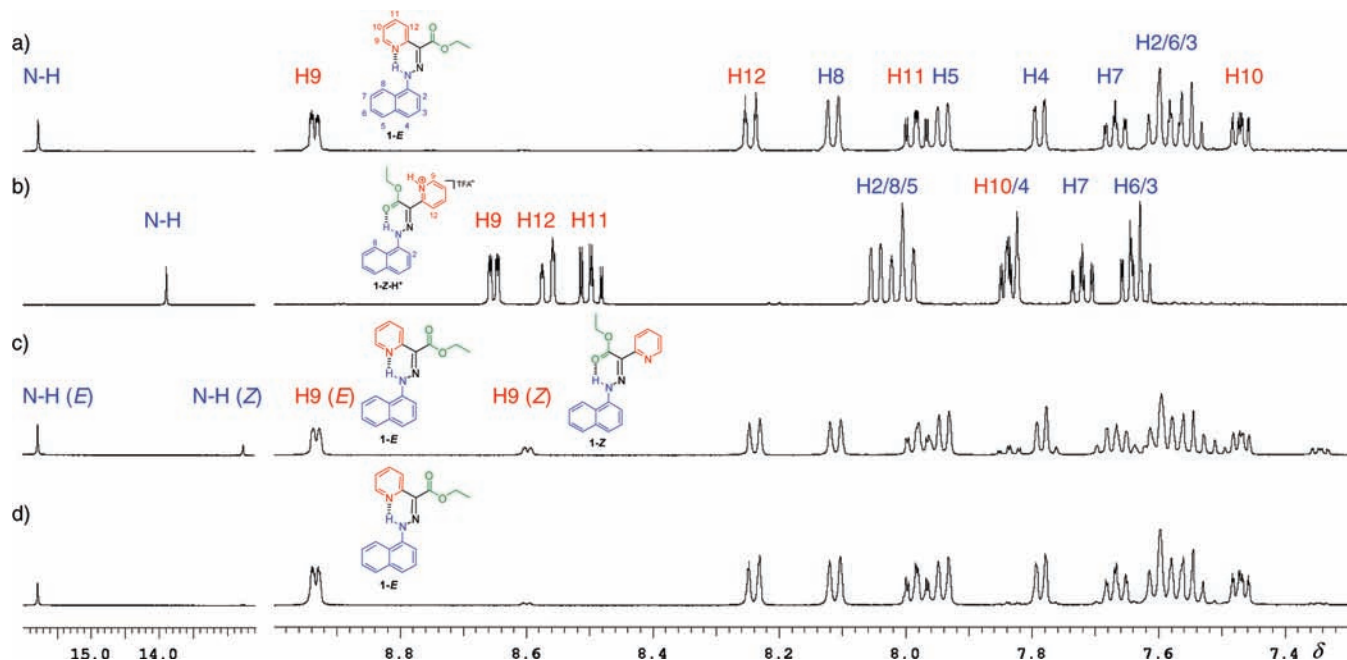


Figure 2. ^1H NMR spectra (500 MHz) in CD_3CN of (a) **1-E** with peak assignments; (b) **1-Z-H⁺** with peak assignments, recorded after the addition of 1.4 equiv of TFA to **1-E**; (c) a mixture of **1-E** and **1-Z**, taken after passing **1-Z-H⁺** over a plug of K_2CO_3 ; and (d) **1-E** after the mixture equilibrated for 2 h at RT.

The addition of 1.4 equiv of $\text{CF}_3\text{CO}_2\text{H}$ (TFA) to a CD_3CN solution of **1-E** results in the protonation of the pyridine subunit,¹⁸ which is accompanied by a color change of the solution from light yellow to orange and drastic changes in the ^1H NMR spectrum (Figure 2b). First of all, the N–H proton signal at 15.8 ppm disappears and a new signal appears at 13.9 ppm (Figure 2b). This shift indicates that a rotation around the $\text{C}=\text{N}$ bond has occurred (*E/Z* isomerization) and that the N–H proton is now H-bonded to the carbonyl group of the ester subunit, yielding **1-Z-H⁺** (Scheme 1). Second, the pyridine proton signals are shifted to lower field, which is a general trend for protonated pyridine rings.¹⁹ The pyridine proton H9 signal has shifted upfield to 8.6 ppm, since it is further away from the naphthalene core and, hence, less affected by its aromatic ring current.²⁰ Proton H2 of the naphthalene subunit is also shifted downfield, which is in accordance with the pyridine ring being protonated. The 2D NOESY spectrum shows a correlation between the N–H and H8 protons (see Figure S5 in the Supporting Information), indicating that in the protonated state the rotamer depicted as **1-Z-H⁺** (Scheme 1) is the predominant one. Moreover, NOE correlations are observed (see Figure S6 in the Supporting Information) between pyridine proton H12 and naphthalene proton H2. This indicates that in the protonated state the pyridinium ion adopts a conformation in which the protonated nitrogen is directed further away from the naphthalene ring, as depicted in **1-Z-H⁺**. When the pyridinium proton H9 is irradiated a correlation is observed between proton H10 and a resonance at 4.1 ppm (see Figure S7a in the Supporting Information). The ^1H NMR spectrum of **1-Z-H⁺** (see Figure S7b in the Supporting Information) shows the presence of a large and broad signal at 4.1 ppm, presumably resulting from excess TFA. The observed correlation can be interpreted to be an interaction between pyridinium H9 and $\text{N}^+\text{–H}$ protons, which means that the latter either is hiding underneath or is in dynamic exchange with the TFA resonance.

Upon passing the CD_3CN solution of **1-Z-H⁺** over a plug of K_2CO_3 or the addition of 1.4 equiv of triethylamine (Et_3N), the color of the solution changes back to light yellow. The ^1H NMR

spectrum (Figure 2c), immediately after passing the solution over K_2CO_3 , shows the complete disappearance of **1-Z-H⁺** and the presence of both **1-E** and **1-Z** in solution. This is evident from the disappearance of the H-bonded N–H peak at 13.9 ppm (Figure 2c) and the appearance of two H-bonded N–H peaks at 15.8 and 12.8 ppm, which are assigned to **1-E** and **1-Z**, respectively. The H9 protons of **1-E** and **1-Z** can also be seen clearly at 8.9 and 8.6 ppm, respectively. Interestingly, the signals of **1-Z** gradually decrease with time and those of the **1-E** configuration grow in return (see Figure S8 in the Supporting Information).²¹ This process (Scheme 1) is the thermal equilibration between the “metastable” configuration and the stable one, **1-Z** and **1-E**, respectively. This process comes to completion within 2 h at RT, and the system regains its original equilibrium ratio of 97:3.²² We used the N–H signals to follow the change in the *E/Z* isomer ratio as a function of time and then used the data to calculate²³ the isomerization rate and energy barrier at room temperature: $k = (2.7 \pm 0.4) \times 10^{-3} \text{ s}^{-1}$ and $\Delta G_{294\text{K}}^\ddagger = 20.7 \pm 0.2 \text{ kcal/mol}$. When the same process was carried out in toluene- d_8 (see Figure S9 in the Supporting Information), which is a less polar solvent than CD_3CN , the calculated rate was $k = (5.7 \pm 0.5) \times 10^{-5} \text{ s}^{-1}$ and the energy barrier was $\Delta G_{294\text{K}}^\ddagger = 22.9 \pm 0.2 \text{ kcal/mol}$. This difference in rates as a function of solvent polarity is an indication that the *E/Z* interconversion occurs via a rotation around the $\text{C}=\text{N}$ bond,²⁴ as opposed to inversion at that nitrogen.⁸

The acid/base induced *E/Z* isomerization of **1-E** in MeCN can also be studied using UV–vis spectroscopy (Figure 3). Upon titration of the **1-E** solution (Figure 3a) with TFA (Figure 3b), the color of the solution starts changing, and the absorption band centered at $\lambda_{\text{max}} = 392 \text{ nm}$ gradually disappears and a new absorption spectrum evolves. This new spectrum (Figure 3c) has two small bands centered at $\lambda_{\text{max}} = 277$ and 312 nm and a larger one centered at $\lambda_{\text{max}} = 428 \text{ nm}$. Upon the addition of Et_3N (Figure 3d) to the protonated solution, the original spectrum centered at $\lambda_{\text{max}} = 392 \text{ nm}$ is steadily regained, showing that the acid/base switching process is fully reversible (Figure 3e).

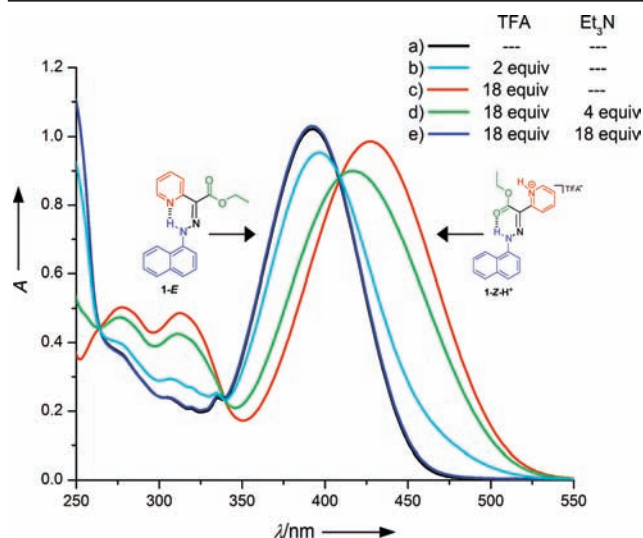


Figure 3. Changes in the UV-vis spectrum during the acid/base switching of **1-E**. All data were recorded in MeCN at 298 K. To a 4.7×10^{-5} M solution of **1-E** (a) TFA was added (b), until there was no observable change (c). Et_3N was then added (d) to switch the system fully back (e). Spectra (a) and (e) are overlapping.

In summary, we have constructed a conceptually new type of chemically induced rotary switch using a hydrazone building block. Unlike previously reported rotary switches this one relies on configurational changes in its function. Various novel applications are conceivable for this system in the future; for example Lewis acids can be used to affect the switching process and thus enable their sensing. Moreover, it is easily possible to exchange the naphthalene ring in this modular switch with other functional groups and even attach it to surfaces, hence allowing its use in logic gate applications^{1d} and drug delivery,^{10f} among others. Currently we are examining these possibilities, in addition to investigating the photochemical switching and the kinetics, thermodynamics, and mechanism associated with the chemical switching process.

Acknowledgment. This work was supported by Dartmouth College and the Burke Research Initiation Award. We wish to thank Drs. David M. Lemal and Amar H. Flood (Indiana University) for helpful discussions, Wayne T. Casey for help with the NMR spectroscopy, Dr. Jaime E. Combariza for help with the calculations, and Dr. Richard Staples (Michigan State University) for help with X-ray analysis.

Supporting Information Available: Experimental procedures, NMR spectra, X-ray crystallographic data for **1-E** (CIF), calculation data, and complete ref 14. This material is available free of charge via the Internet at <http://pubs.acs.org>.

References

- (1) (a) Kottas, G. S.; Clarke, L. I.; Horinek, D.; Michl, J. *Chem. Rev.* **2005**, *105*, 1281–1376. (b) Kay, E. R.; Leigh, D. A.; Zerbetto, F. *Angew. Chem., Int. Ed.* **2007**, *46*, 72–191. (c) Balzani, V.; Credi, A.; Venturi, M. *Molecular Devices and Machines - Concepts and Perspectives for the Nanoworld*; Wiley-VCH: Weinheim, Germany, 2008. (d) Szacitowski, K. *Chem. Rev.* **2008**, *108*, 3481–3548.
- (2) *Molecular Switches*; Feringa, B. L. Ed.; Wiley-VCH: Weinheim, Germany, 2001.
- (3) For some examples, please see: (a) Badjić, J. D.; Stoddart, J. F. *Science* **2004**, *303*, 1845–1849. (b) Berna, J.; Leigh, D. A.; Lubomska, M.; Mendoza, S. M.; Perez, E. M.; Rudolf, P.; Teobaldi, G.; Zerbetto, F. *Nat. Mater.* **2005**, *4*, 704–710. (c) Bonnet, S.; Collin, J. P.; Koizumi, M.; Mobian, P.; Sauvage, J.-P. *Adv. Mater.* **2006**, *18*, 1239–1250.
- (4) *Molecular Motors*; Schilwa, M., Ed.; Wiley-VCH: Weinheim, Germany, 2003.
- (5) By configuration we mean *cis-trans* isomerism around double bonds. See ref 1b.
- (6) Feringa, B. L. *J. Org. Chem.* **2007**, *72*, 6635–6652.
- (7) Parmeter, S. M. In *Organic Reactions*; Adam, R., Ed.; Wiley-VCH: New York, 1959; Vol. 10, p 1.
- (8) McCarthy, C. G. In *The Chemistry of the Carbon-Nitrogen Bond*; Patai, S., Ed.; John Wiley and Sons: New York, 1970; pp 392–399.
- (9) (a) Yao, H. C. *J. Org. Chem.* **1964**, *29*, 2959–2963. (b) Bose, A. K.; Kugajevsky, I. *Tetrahedron* **1967**, *23*, 1489–1497. (c) Karabatsos, G. J.; Taller, R. A. *Tetrahedron* **1968**, *24*, 3923–3937. (d) Mitchell, A. D.; Nonhebel, D. C. *Tetrahedron Lett.* **1975**, *16*, 3859–3862. (e) Mitchell, A. D.; Nonhebel, D. C. *Tetrahedron* **1979**, *35*, 2013–2019. (f) Bertolasi, V.; Ferretti, V.; Gilli, P.; Issa, Y. M.; Sherif, O. E. *J. Chem. Soc., Perkin Trans. 2* **1993**, 2223–2228.
- (10) For examples of pH activated switches, see: (a) Dolain, C.; Maurizot, V.; Huc, I. *Angew. Chem., Int. Ed.* **2003**, *42*, 2738–2740. (b) Keaveney, C. M.; Leigh, D. A. *Angew. Chem., Int. Ed.* **2004**, *43*, 1222–1224. (c) Cheng, K.-W.; Lai, C.-C.; Chiang, P.-T.; Chiu, S.-H. *Chem. Commun.* **2006**, 2854–2856. (d) Silvi, S.; Arduini, A.; Pochini, A.; Secchi, A.; Tomasulo, M.; Raymo, F. M.; Baroncini, M.; Credi, A. *J. Am. Chem. Soc.* **2007**, *129*, 13378–13379. (e) Uchiyama, S.; Iwai, K.; de Silva, A. P. *Angew. Chem., Int. Ed.* **2008**, *47*, 4667–4669. (f) Angelos, S.; Yang, Y.-W.; Khashab, N. M.; Stoddart, J. F.; Zink, J. I. *J. Am. Chem. Soc.* **2009**, *131*, 11344–11346.
- (11) No change was observed in the ^1H NMR spectrum of **1-E** upon the addition of 1.0 equiv of Et_3N or K_2CO_3 to the solution. Upon the addition of 0.1 equiv of acid (TFA) only the appropriate amount of isomerization occurred. This rules out the catalytic equilibration process observed in other 1,2,3-tricarbonyl-2-arylhydrazone systems.
- (12) These types of hydrazones usually adopt planar structures. For other examples, see: (a) Vickery, B.; Willey, G. R.; Drew, M. G. B. *J. Chem. Soc., Perkin Trans. 2* **1981**, 155–160. (b) Drew, M. G. B.; Vickery, B.; Willey, G. R. *Acta Crystallgr., Sect. B* **1982**, *38*, 1530–1535. (c) Frohberg, P.; Drutkowski, G.; Wagner, C. *Eur. J. Org. Chem.* **2002**, 1654–1663.
- (13) This isomer ratio remained constant even after heating the sample at 55 °C for 1 h.
- (14) Frisch, M. J.; et al. *Gaussian 03*, revision B.04; Gaussian Inc.; Wallingford, CT, 2004.
- (15) (a) Becke, A. D. *J. Chem. Phys.* **1993**, *98*, 5648–5652. (b) Lee, C.; Yang, W.; Parr, R. G. *Phys. Rev. B* **1988**, *37*, 785–789.
- (16) Dunning, T. H., Jr. *J. Chem. Phys.* **1989**, *90*, 1007–1023.
- (17) The reason for this is most probably the unfavorable interaction between proton H8 and the C=N nitrogen lone pair in the other conformation.
- (18) The addition of 1.4 equiv of TFA yields 98% pyridine protonation. For full protonation, 2.0 equiv are required. Only 1.0 equiv of TFA is needed to fully protonate the starting material, ethyl-2-pyridylacetate. The H-bonding with the N–H proton and the conjugation with the aromatic system apparently decrease the basicity of the pyridine nitrogen in **1-E**. Subsequently, when $\text{CH}_3\text{SO}_3\text{H}$ is used as the acid, only 1.0 equiv is needed to fully protonate the pyridine subunit.
- (19) *Tables of Spectral Data for Structure Determination of Organic Compounds*; Pretsch, E., Ed.; Springer-Verlag: Berlin, Germany, 1989; Vol. 2.
- (20) In ethyl-2-pyridylacetate this same proton resonates at 8.5 ppm and shifts to 8.7 ppm upon protonation with TFA. This indicates that the shift to 8.9 ppm in **1-E** has to do with the aromatic ring current. In **1-Z** proton H9 resonates at 8.6 ppm (*vide infra*), which is in agreement with the pyridine ring being further away from the naphthalene core. This is again in agreement with **1-E** being the predominant configuration in solution.
- (21) When Et_3N is added to the solution, the fully equilibrated spectrum is generated instantaneously and this process is not observed. The reason for this might be the larger contact time the solution has with Et_3N .
- (22) This complete switching cycle was repeated 5 times in CD_3CN , using TFA as acid and Et_3N as the base, and the same switching behavior was observed over the 5 switching runs.
- (23) Connors, K. A. *Chemical Kinetics: The Study of Reaction Rates in Solution*; John Wiley and Sons, Inc.: New York, 1990; pp 60–61.
- (24) (a) Tobin, J. C.; Hegarty, A. F.; Scott, F. L. *J. Chem. Soc. B* **1971**, 2198–2202. (b) Wong, J. L.; Zady, M. F. *J. Org. Chem.* **1975**, *40*, 2512–2516. (c) Pichon, R.; Le Saint, J.; Courtot, P. *Tetrahedron* **1981**, *37*, 1517–1524.

JA909149Z